Synthesis, Characterization, and Catalytic Activity of Mesostructured Titanosilicates Assembled from Polymer Surfactants with Preformed Titanosilicate Precursors in Strongly Acidic Media

Xiangju Meng, Defeng Li, Xiaoyu Yang, Yi Yu, Shuo Wu, Yu Han, Qing Yang, Dazhen Jiang, and Feng-Shou Xiao*

State Key Laboratory of Inorganic Synthesis and Preparative and Chemistry & Department of Chemistry, Jilin University, Changchun 130023, P. R. China

Received: November 7, 2002; In Final Form: June 3, 2003

Novel mesostructured titanosilicates designated as MTS-9 have been successfully synthesized from assembly of preformed nanosized titanosilicate precursors with polymer surfactants. Mesoporous MTS-9 shows highly hydrothermal stability in boiling water (over 120 h) as compared with that of Ti−MCM-41 and SBA-15. In phenol hydroxylation, Ti−MCM-41 shows very low catalytic activity (2.5%), but MTS-9 exhibits very high catalytic activity, with phenol conversion of 26%, which is comparable with TS-1. In styrene epoxidation, MTS-9 shows high activity and selectivity similar to those of TS-1, which are much different from those of Ti−MCM-41. In 2,3,6-trimethylphenol hydroxylation, Ti−MCM-41 is inactive because of the relatively low oxidation ability of Ti species in the amorphous wall of Ti−MCM-41, and TS-1 is also inactive because of the inaccessibility of the small micropores of TS-1 to the large diameter of a bulky molecule like 2,3,6-trimethylphenol. However, MTS-9 is very active for this reaction with conversion of 18.8% indicating that MTS-9 is an effective catalyst for the oxidation of bulky molecules. The MTS-9 samples were characterized with infrared, UV−visible, UV−Raman, and numerous other techniques. The results suggest that the titanium species in MTS-9 are TS-1-like, and that the pore walls of MTS-9 contains primary and secondary structural building units, similar to those of microporous zeolites. Such unique structural features might be responsible for the observed strong oxidation ability and high hydrothermal stability of the mesostructured titanosilicates. Heating MTS-9 at 500 °C leads to the transformation of titanium species, giving relatively low catalytic conversion in phenol hydroxylation, which suggests that increasing thermal stability of titanium sites like TS-1 species in the mesoporous wall is still a great task for preparation of mesostructured titanosilicates.

1. Introduction

Oxidation reactions are very important industrial processes for production of fine chemicals in organic synthesis, and currently there are great interests in titanium-containing zeolitic catalysts for selective oxidations. Since the discovery of microporous crystal of TS-1 by Enichem Company,[1] a series of microporous titanosilicates have been reported such as Ti−ZSM-12,[2] Ti−ZSM-48,[3] and Ti−Beta.[4] All of these titanosilicates show remarkable catalytic properties.[1−7] One disadvantage of these titanosilicate catalysts is that their pore sizes (generally less than 8 Å) are too small to allow bulky reactants access to the active sites in the micropores of the zeolite, while the bulky reactants dominate most of the chemical transformations which are of central importance in the fine chemical and pharamaceutical industries. Therefore, novel porous titanosilicates with larger pore size have always been sought.

Mesoporous materials were first discovered by Mobil scienctists in 1992,[8] which offers a new route for preparation of ordered mesoporous titanosilicates with pore size of 30∼200 Å. Ti−MCM-41 is the first example for ordered mesoporous titanosilicates, and catalytic results exhibit good properties for the oxidation of bulky reactants under mild conditions, but unfortunately, compared with TS-1, the oxidation ability and hydrothermal stability are relatively low.[9,10]

There have been several successful examples for the preparation of mesoporous titanosilicates that have reasonably good hydrothermal stability or catalytic activity.[11−15] As examples, mesoporous Ti−SBA-15 with thick pore walls have been prepared using triblock copolymers as templates.[11] The synthesis of Ti−HMS and Ti−MSU materials have been achieved using neutral surfactants as the templates.[12] Through the grafting route, titanocene complex onto mesoporous silica exhibit high activity for catalytic conversion of bulky molecules.[13,] Despite encouraging progress in recent years, both the hydrothermal stability and oxidation ability of the current mesoporous titanosilicates are yet generally lower than those of microporous titanosilicate zeolites. The relatively low oxidation ability in catalysis and hydrothermal stability can be attributed to the amorphous nature of the mesoporous wall.[16] The coordination environment of Ti species in amorphously mesoporous wall is quite different from that of TS-1[1] and gives relatively low catalytic activity as compared with 4-coordinated titanium species in TS-1 zeolite. Therefore, novel mesoporous titanosilicates with TS-1-like titanium species and high catalytic oxidation ability are still desirable.

More recently, there has been great progress in the preparation of mesostructured materials assembled from nanoclusters, such as mesostructured metal germanium sulfides[17] and mesoporous aluminosilicate nanoclusters.[18−20] Particularly, the surfactant micelle assemble with aluminosilicate nanoclusters in basic

* To whom correspondence should be addressed. Fax: 86/431-5671974; e-mail: fsxiao@mail.jlu.edu.cn.

10.1021/jp027405l CCC: $25.00
Published on Web 07/17/2003

media to form hydrothermally stable and strongly acidic ordered mesoporous aluminosilicates as compared with those of MCM-41.[19] In these mesoporous aluminosilicates, aluminum species in mesoporous wall are zeolite-like, exhibiting similar acidic properties to those of aluminosilicate zeolites. Furthermore, the assembly of surfactant micelle with zeolite nanoclusters is applied to strongly acidic media,[20] and it is found that, as compared with basic media, the strong acidic media show obvious advantages in the following: (1) the growth of microporous crystals is avoided, because microporous crystals cannot be crystallized in strongly acidic media; (2) the appearance of TiO_2 as a separate phase is avoided. Generally, the TiO_2 phase, which easily forms under basic conditions used in the preparation of porous titanosilicates such as TS-1 and Ti−MCM-41, is often active in the nonproductive H_2O_2 decomposition in oxidation reactions.

In our preliminary work, we have briefly reported the synthesis of an ordered mesoporous titanosilicate (MTS-9) by the assembly of preformed titanosilicate precursors with triblock copolymers in a strong acidic media.[20,21] We demonstrate here the detailed results of synthesis, structure, characterization, and excellent catalytic activity of MTS-9 in the oxidation of the small molecules of phenol and styrene and also of the bulky molecule of 2,3,6-trimethylphenol.

2. Experimental Section

2.1. Materials. Titanium tetrabutoxide (TBOT), tetraethyl orthosilicate (TEOS), ethanol and hydrochloric acid, phenol, catechol, hydroquinone, benzoquinone, benzaldehyde, phenylacetaldehyde, styrene, 2,3,6-trimethylphenol, trimethylhydroquinone, trimethylbenzoquinone, and H_2O_2 (30%) were purchased from Beijing Chemical Co. $EO_{20}PO_{70}EO_{20}$ (Pluronic P123) are Aldrich products, tetrapropylammonium hydroxide (TPAOH) and styrene epoxide were purchased from Fluka chemical Co.

2.2. Synthesis. The ordered mesoporous tianosilicates were synthesized from assembly of polymer surfactant micelle with preformed titanosilicate precursors in strongly acidic media.[20,21] As a typical example, the synthesis for MTS-9 is as follows: (1) The zeolite precursors solution with zeolite TS-1 primary structure units were prepared by mixing 6 mL of TPAOH aqueous solution (25%) with 12 mL of H_2O, followed by addition of 0.3 mL of $Ti(OC_4H_9)_4$ and 5.6 mL of TEOS under stirring ($TiO_2/SiO_2/TPAOH/C_2H_5OH/H_2O$ molar ratios of 1.0/30/8/120/1500). The mixture is then aged at 45 °C for 2−4 days. The final product is also a clear solution. (2) $EO_{20}PO_{70}EO_{20}$ (0.8 g) (Pluronic P123) was dissolved in 20 mL of H_2O mixed with 5 mL of HCl (10 M/L), followed by addition of 9.0 mL of precursor solution (containing 8 mmol of SiO_2) obtained in step 1. The mixture was stirred at 40 °C for 20 h, then transferred into an autoclave for additional reaction at 100 °C for 24 h. (3) The product prepared from the titanosilicate precursors was collected by filtration, washed several times, and dried in air. By these procedures, most of the templates of polymer surfactant (P123) in the mesopores were removed, but the templates of small molecules of TPA^+ were still in the mesoporous wall. Such products are defined as as-synthesized MTS-9. (4) As-synthesized MTS-9 was calcined at 500 °C for 4 h to remove the residual template of TPA^+, and calcined MTS-9 do not have any organic templates.

The samples of Ti−MCM-41, Ti−HMS, SBA-15, and Ti−SBA-15 were prepared according to literature.[10−12]

2.3. Characterization. X-ray diffraction patterns were obtained with a Siemens D5005 diffractometer using Cu Kα radiation. Transmission electron microscopy images were recorded on JEOL 2010F and Philips CM200FEG with an acceleration voltage of 200 kV. The isotherms of nitrogen were measured at the temperature of liquid nitrogen using a Micromeritics ASAP 2010M system. The samples were outgassed for 10 h at 300 °C before the measurements. The pore-size distribution was calculated using the Barrett−Joyner−Halenda (BJH) model. UV−vis spectra were measured with spectrometer of PE Lambda 20, and $BaSO_4$ was an internal standard sample. UV−Raman spectra were recorded on a UV−Raman spectrometer built by the State Key Laboratoty for catalysis, Dalian Insitute of Chemical Physics, Dalin, China. The UV line excited at 244 nm was from a Coherent Ionva 300 Fred ultraviolet laser instrument equipped with an intracavity frequency-doubling system based on a β-barium borate (BBO) crystal. The laser power at the sample was kept below 4.0 mw. At 180 °C, collection geometry was used to collect the scattered Raman light. The spectra resolution was estimated to be 1.0 cm^{-1}. Powders of samples were pressed into pellets with diameters of 1.0 cm and placed in a sample holder.

2.3. Catalytic Tests. Phenol hydroxylation experiments were run in a 50-mL glass reactor and stirred with a magnetic stirrer. In a standard run, 13.6 mmol of phenol, 50 mg of catalyst, and 10 mL of solvent were mixed, followed by addition of 4.53 mmol of H_2O_2 (30% aqueous). After the reaction for 4 h at 353 K, the products were hydroquinone (HQ), catechol (CAT), and 1,4-benzoquinone (BQ), which were analyzed by gas chromatography (GC-9A, Shimadzu, using Flame Ionization Detector) with flexible quartz capillary column coated with OV-17. The initially programmed temperature was 100 °C, the final temperature was 180 °C, and the injector temperature was 280 °C.

The epoxidation of styrene was performed in a 50-mL glass reactor and stirred with a magnetic stirrer. In a standard run, 17.4 mmol of styrene, 10 mL of acetone as solvent, and 90 mg of catalyst were mixed in the reactor and heated to a given temperature. Then, 5.8 mmol of H_2O_2 (30% aqueous) was added into the reactor. After the reaction for 3 h at 318 K, the product were taken out from the system and analyzed by gas chromatography (GC-17A, Shimadzu, using Flame Ionization Detector) with a flexible quartz capillary column coated with OV-1.

The hydroxylation of 2,3,6-trimethylphenol was performed in a 50-mL glass reactor and stirred with a magnetic stirrer. In a standard run, 7.3 mmol of 2,3,6-trimethylphenol, 2.5 mL of acetone as solvent, and 50 mg of catalyst were mixed in the reactor and heated to a given temperature. Then, 2.78 mmol of H_2O_2 (30% aqueous) was added into the reactor. After the reaction for 2 h at 353 K, the product were taken out from the system and analyzed by gas chromatography (GC-17A, Shimadzu, using Flame Ionization Detector) with a flexible quartz capillary column coated with OV-1.

3. Results

3.1. X-ray Diffraction. Figure 1 shows the small-angle X-ray diffraction patterns of as-synthesized MTS-9, calcined MTS-9, and calcined MTS-9 treated by boiling water for 120 h. As-synthesized MTS-9 sample (Figure 1A) clearly shows that three peaks indexed as (100), (110), and (200), which can be associated with the hexagonal symmetry. The (100) peak reflects a d spacing of 112 Å (a_0 = 130Å). After calcination in air at 500 °C for 4 h, the sample XRD pattern (Figure 1B) shows that the three diffraction peaks are still present, confirming that hexagonal MTS-9 is thermally stable. A similarly high degree of mesoscopic order is observed for hexagonal MTS-9 even after calcination to 800 °C. Particularly, after treatment of

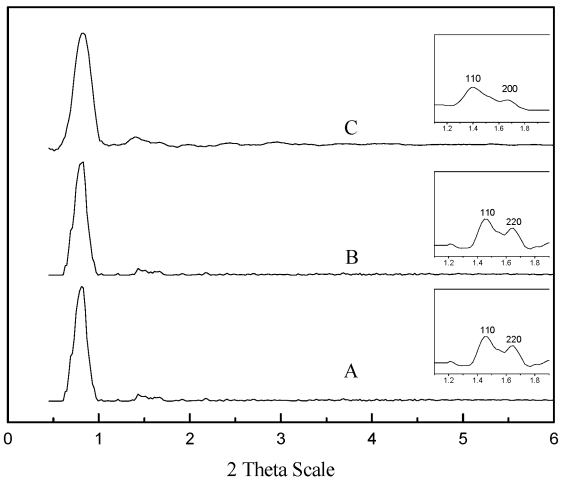

Figure 1. The small-angle X-ray diffraction patterns of (A) as-synthesized MTS-9, (B) calcined MTS-9, and (C) MTS-9 treated by boiling water for 120 h.

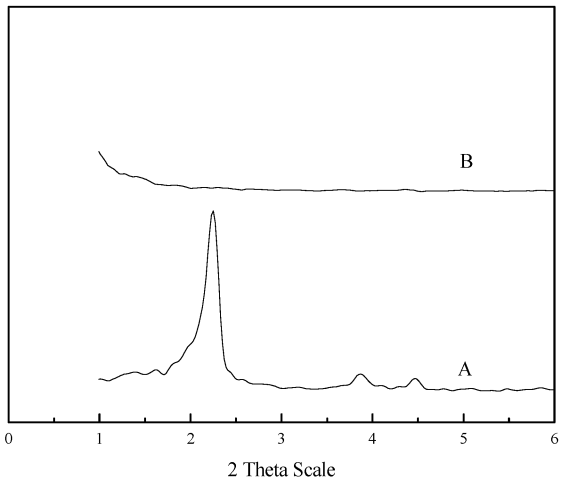

Figure 2. The small-angle X-ray diffraction patterns of (A) SBA-15 and (B) SBA-15 treated by boiling water for 120 h.

calcined MTS-9 sample in boiling water for 120 h, the XRD pattern of MTS-9 (Figure 1C) also shows characteristic peaks assigned with hexagonal symmetry, indicating that hexagonal MTS-9 has remarkable hydrothermal stability. Furthermore, no diffraction peak was observed in the region of higher angles 10−40° for MTS-9, which indicates the absence of large microporous crystals in the sample, suggesting that MTS-9 sample is a pure phase.

Figures 2 and 3 show the small-angle X-ray diffraction patterns of SBA-15 and Ti−MCM-41, respectively. Both Ti−MCM-41 and SBA-15 show obvious peaks assigned to hexagonal symmetry, and the (100) peak of Ti−MCM-41 and SBA-15 reflects the *d* spacing of 41.6 Å (a_0 = 48.1Å) and 92 Å (a_0 = 106Å). However, after the treatment of boiling water for 120 h, both Ti−MCM-41 and SBA-15 lost most of their mesostructure, suggesting their relatively low hydrothermal stability.

3.2. N_2 Adsorption Isotherms. Figure 4 shows N_2 adsorption−desorption isotherms of as-synthesized MTS-9 and SBA-15 before and after treatment by boiling water for 120 h, and the parameters for N_2 adsorption−desorption of MTS-9, Ti−MCM-41, and SBA-15 are presented in Table 1. Notably, as-synthesized MTS-9 (Figure 4A) and SBA-15 (Figure 4B) show the same isotherms of type IV. A step increasing occurs in the curve at a relative pressure $0.7 < P/P_0 < 0.8$, which is due to the mesoporous structures. Correspondingly, pore size distribution for MTS-9 and SBA-15 shows narrow uniform mesopores at the mean values of 80 and 72 Å, respectively; the surface area for MTS-9 and SBA-15 exhibits at 980 and 870 m^2/g, respectively (Table 1).

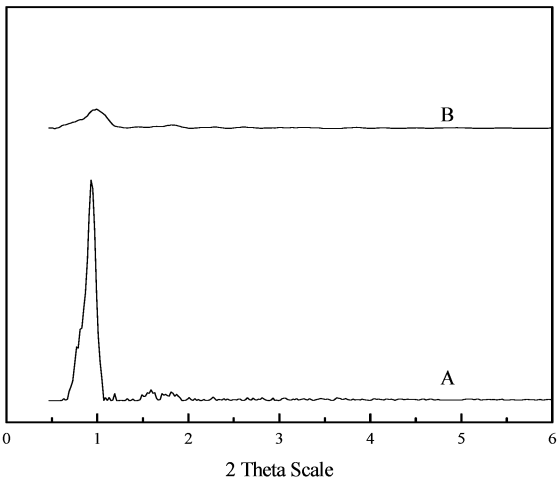

Figure 3. The small-angle X-ray diffraction patterns of (A) Ti−MCM-41 and (B) Ti−MCM-41 treated by boiling water for 120 h.

Interestingly, after treatment by boiling water for 120 h, only MTS-9 keeps its mesostructure and gives BET surface area and BJH pore size at 720 m^2/g and 8.9 nm, respectively. In contrast, SBA-15 and Ti−MCM-41 lost their mesostructure, giving the surface area only at 187 and 55 m^2/g, respectively (Table 1). These results are good in agreement with the XRD patterns of the samples, which confirm the high hydrothermal stability of MTS-9.

Figure 4E shows N_2 adsorption−desorption isotherms of calcined MTS-9. The isotherm shows typical adsorption curve of type IV plus type I. A steep increasing occurs in the curve at a relative pressure $10^{-6} < P/P_0 < 0.01$, which is due to the filling of micropores. Another step can be identified in the adsorption curve at a relative pressure $0.7 < P/P_0 < 0.8$, which is due to the mesoporous structures. Correspondingly, pore size distribution for calcined MTS-9 shows two narrow uniform pores at the mean values of 5.3 and 80 Å assigned to micropores and mesopores, respectively. Furthermore, we observe that the surface area and pore volume of calcined MTS-9 is higher than those of SBA-15, which are assigned to the contribution of micropores in mesoporous wall.

Figure 5 shows the *t*-plots of as-synthesized and calcined MTS-9 sample, respectively. Generally, the *t*-plots of conventional mesoporous materials should pass zero of axis, meaning no micropores in them. However, calcined sample shows micropore volume at 0.15 cm^3/g, which is possibly assigned to the removal of organic template of TPAOH, because as-synthesized samples washed by water and ethanol can only remove the polymer surfactants, and the smaller template of TPAOH is still in the samples. The existence for larger micropore volume in MTS-9 may also be attributed to the existence of zeolite MFI primary units in the mesoporous walls.

3.3 Transmission Electron Microscopy. TEM image of MTS-9 (Figure 6) exhibits hexagonal arrays of mesopores with uniform pore size. The corresponding ED pattern also shows reflections consistent with hexagonal symmetry. From high-dark contrast in the TEM image of the sample, the distance between mesopores is estimated to be 120 Å. Furthermore, we observed that the wall thickness of MTS-9 is greater than that of SBA-15 reported in the literature, which is well consistent with the result characterized by XRD and N_2 adsorption experiments.

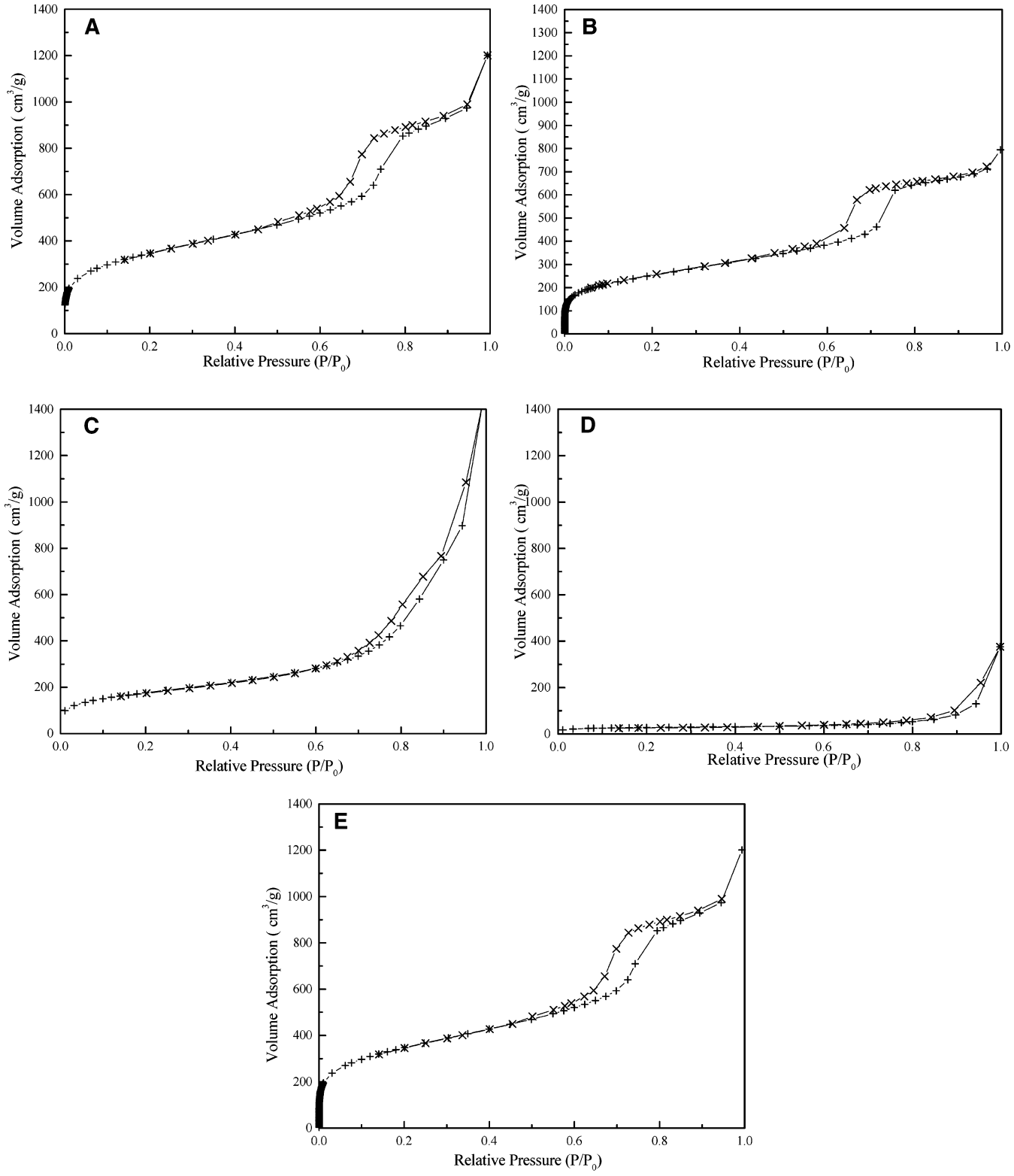

Figure 4. (A) Nitrogen adsorption (+)−desorption (×) isotherm for as-synthesized MTS-9; (B) nitrogen adsorption (+)−desorption (×) isotherm for as-synthesized SBA-15; (C) nitrogen adsorption (+)−desorption (×) isotherm for MTS-9 treated by boiling water for 120 h; (D) nitrogen adsorption (+)−desorption (×) isotherm for SBA-15 treated by boiling water for 120 h; (E) nitrogen adsorption (+)−desorption (×) isotherm for calcined MTS-9.

Figure 7 shows HR TEM image of MTS-9, corresponding to area B in Figure 6. Obviously, some micropores 4−5 Å in diameter are observed.[22] This further confirms the presence of microporosity in the mesoporous materials. More importantly, micropore arrays with more or less periodicity in the mesoscale pore wall are found. These microporous arrays are mostly around 2 nm in size (marked area in Figure 7).[22] In contrast, we cannot observe microporous arrays in mesoporous wall of SBA-15, although we easily find obvious micropores in the wall, in good agreement with previous report.[22]

3.4 IR Spectroscopy. Figure 8 gives the mid-infrared spectra of SBA-15 and MTS-9. IR spectrum of SBA-15 shows a broad band at 460 cm^{-1} in the region of 400−600 cm^{-1}, which is similar to those of amorphous materials. However, MTS-9

TABLE 1: The Parameters over Calcined MTS-9, Ti-MCM-41, and SBA-15 Samples before and after Treatment in Boiling Water for 120 h

sample	pore size (nm)	wall thickness (nm)	total pore volume (cm^3/g)	micropore volume (cm^3/g)	total surface area (m^2/g)	micropore surface area (m^2/g)	mesopore surface area (m^2/g)
MTS-9	8.0	4.8	1.35	0.15	980	380	600
treated	8.9	4.3	1.40	0.10	720	136	584
Ti-MCM-41	2.7	1.5	0.73		1080		1080
treated					55		55
SBA-15	7.2	3.6	1.05	0.05	870	315	555
treated					187		187

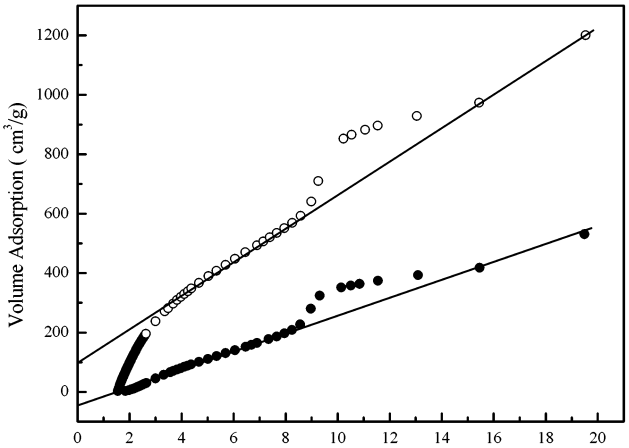

Figure 5. *t*-plots of as-synthesized and calcined MTS-9.

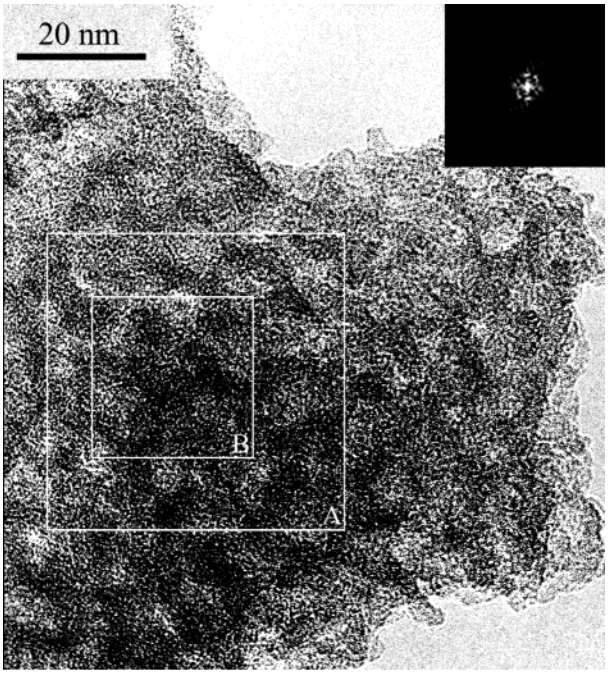

Figure 6. (A) Transmission electron microscopy (TEM) image of calcined MTS-9, (B) beam electron diffraction of calcined MTS-9 for mesopores.

exhibits an obvious band at 556 cm^{-1} in addition to the band at 460 cm^{-1}. The band at 556 cm^{-1} is similar to that of five-membered rings of T−O−T (T = Si or Al) in microporous zeolites.[23] The results suggest that MTS-9 has zeolite primary and secondary building units.

Furthermore, the preparation of titanosilicate precursors from TPAOH has also been monitored with IR spectroscopy. When Ti $(OC_4H_9)_4$ was mixed with silica in the presence of TPAOH solution at room temperature, IR spectrum does not show the bands at 520−600 cm^{-1} assigned to five-membered rings of T−O−T. After heating the titanosilicate gel in the presence of

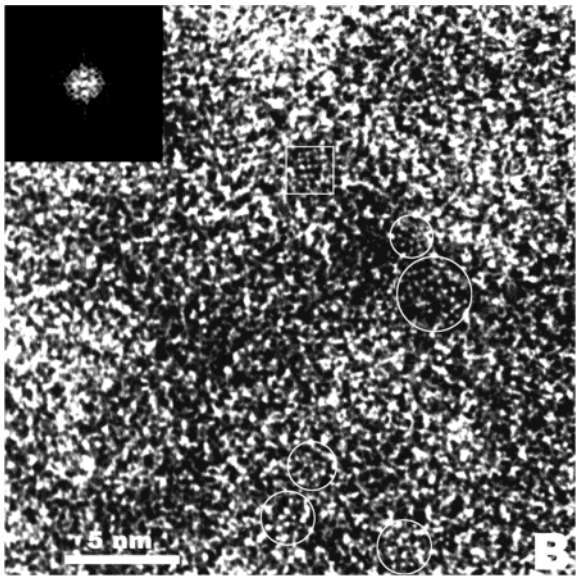

Figure 7. Enlarged HR TEM image of MTS-9, corresponding to area B in Figure 8.

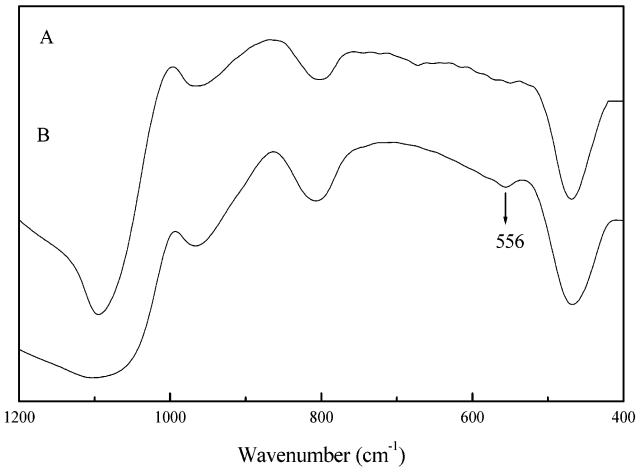

Figure 8. Mid-infrared spectra of (A) SBA-15 and (B) MTS-9.

TPAOH at 140 °C for several hours, the precursors for preparing MTS-9 are formed, which give rise to a band (520−600 cm^{-1}) centered at 550 cm^{-1} (Figure 9), indicating the existence of zeolite TS-1 primary and secondary building units in these precursors. In contrast, the same treatment for the titanosilicate gel in the absence of TPAOH does not cause the appearance of this band.

3.5 UV−Visible Spectroscopy. UV−visible spectroscopy is a very common method for characterization of coordination condition of Ti in zeolite framework.[16,24] The spectra of Ti−MCM-41 and MTS-9 samples are shown in Figure 10. MTS-9 has an obvious adsorption band at 215 nm, which is very similar to that of TS-1, assigned to the titanium species in T_d coordination. The absence of a band at 330 nm implies that anatase

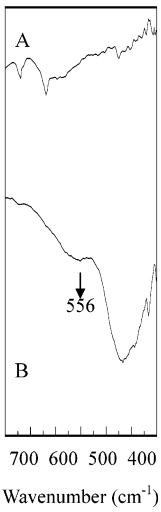

Figure 9. IR spectra recorded during the preparation of titanosilicate precursors: (A) Ti species were mixed with silica in the presence of TPAOH solution at room temperature; (B) after the step in (A) the mixture gel was heated at 140 °C for 2−3 h.

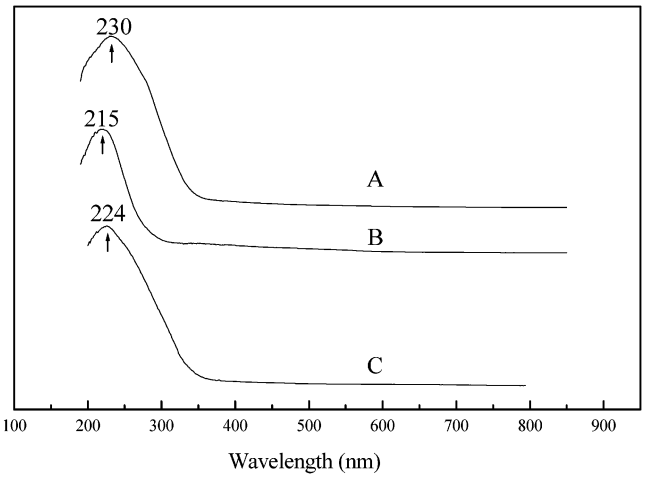

Figure 10. UV−visible spectra of (A) Ti−MCM-41, (B) MTS-9, and (C) calcined MTS-9.

phase is not present, because of the strong acidic condition preventing the formation of TiO_2. In contrast, the UV−vis spectrum of Ti−MCM-41 shows very broader adsorption band centered at 230 nm (Figure 10B), which is assigned to Ti species in the amorphous nature with coordination number between 4 and 6. These results indicate that the nature of titanium coordination between Ti−MCM-41 and TS-1 is distinguishable.

When MTS-9 is calcined at 500 °C for 4 h, the sample UV−vis spectrum exhibits adsorption band at 224 nm (Figure 10C), which shifts to higher several nanometers. Corma has concluded[16] that a sample containing only framework titanium would give an optical transition at 210 nm, which is assigned to a charge transfer (CT) in $[TiO_4]$ and $[O_3Ti-OH]$ moieties (Ti species in TS-1 sample), and isolated extraframework hexacoordinated Ti would give a CT at about 225 nm (most of Ti species in mesostructured titanosilicates). The spectra shifts to higher band indicate that Ti species in MTS-9 samples is similar to the former (TS-1) before calcinations and transformed into the latter (Ti−MCM-41) after calcinations.

3.6 UV−Raman Spectroscopy. UV−Raman spectroscopy is very sensitive to the coordination environment of titanium species. The framework titanium ions of TS-1 have been identified with UV−Raman spectroscopy by the asymmetric stretching of Ti−O−Si species, and the asymmetric stretching

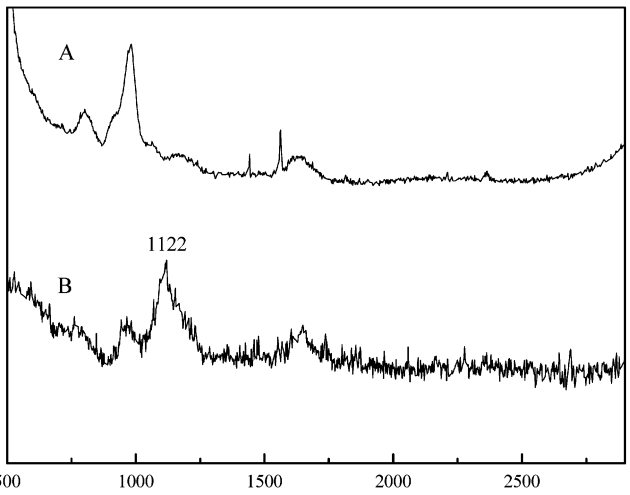

Figure 11. UV−Raman spectra of (A) Ti−MCM-41 and (B) MTS-9.

TABLE 2: Catalytic Activities in Phenol Hydroxylation over MTS-9, Ti-MCM-41, and TS-1[a]

catalysts	phenol conversion (%)	TOF (h^{-1})	product selectivity (%)		
			CAT	HQ	BQ
MTS-9	26.3	6.8	59.5	39.8	0.7
Calcined MTS-9	14.5	4.0	53.2	45.7	1.1
Ti-MCM-41	2.5	0.5	60.1	38.0	1.9
Ti-HMS[c]	0.5	0.1	58.5	41.5	0.5
TS-1[d]	28.0	5.5	50.4	48.6	1.0

[a] Reaction conditions: water as a solvent, reaction temperature at 80 °C, phenol/H_2O_2 = 3/1 (molar ratio), reaction time for 4 h, catalyst/phenol = 5% (weight ratio). CAT = catechol, HQ = hydroquinone, BQ = benzoquinone. The product of tar is not included. [b] The sample was heating at 500 °C for 4 h. [c] Ti−HMS with Si/Ti ratio of 30 was synthesized according to published procedure.[12] [d] TS-1 with Si/Ti ratio of 30 was synthesized according to published procedure.[1]

vibration mode of the tetrahedral framework titanium of TS-1 is 1125 cm^{-1}.[25] Figure 11 shows the spectra of the MTS-9 and Ti−MCM-41 samples, exhibiting bands at 1122 and 1110 cm^{-1}. The band at 1122 cm^{-1} in the spectrum of MTS-9 is very close to that of TS-1 (1125 cm^{-1}), indicating that the chemical environment of Ti species in MTS-9 is very close to that of TS-1. On the contrary, the band at 1110 cm^{-1} in Ti−MCM-41 shifted to lower frequency as compared with MTS-9 and TS-1. The shift to lower frequency is interpreted that Ti species in Ti−MCM-41 are loosely coordinated to the Si atoms in the framework.[29] Therefore, it is suggested that the bonding of Ti−O−Si is more loosely than that of TS-1, which is obviously distinguishable to those of MTS-9 and TS-1.

3.7 Catalytic Results. *Phenol Hydroxylation.* The catalytic activities of various titanosilicates in phenol hydroxylation are presented in Table 2. Notably, MTS-9 and TS-1 exhibit excellent activity, giving the conversion at 26.3 and 28.0%, respectively. In contrast, Ti−MCM-41 and Ti−HMS show relatively low conversion at 2.5 and 0.5%, respectively. The big difference in catalytic activity between MTS-9 and TS-1 with Ti−MCM-41 and Ti−HMS is reasonably attributed to the distinguished titanium species in these titanosilicates. Microporous crystal of TS-1 is a well-known good catalyst for phenol hydroxylation, but there is no report yet that mesoporous titanosilicates such as MTS-9 exhibit relatively high catalytic activity in this reaction. The very low conversion in phenol hydroxylation over mesoporous titanosilicates of Ti−MCM-41 and Ti−HMS is due to relatively low oxidation ability of titanium species in amorphous nature of mesoporous wall.[16]

TABLE 3: Catalytic Activities in Styrene Epoxidation over MTS-9, Ti-MCM-41, and TS-1[a]

catalysts	styrene conversion (%)	TOF (h^{-1})	product selectivity (%)		
			styrene epoxide	phenyl-acetaldehyde	benz-aldehyde
MTS-9	56.4	9.4	28.0	29.3	42.7
Ti-MCM-41	48.3	6.1			100
TS-1[b]	54.6	5.2	13.3	58.3	29.0

[a] Reaction conditions: Aceton as a solvent, reaction temperature at 45 °C, styrene/H_2O_2 = 3/1 (molar ratio), reaction time for 5 h, catalyst/phenol = 5% (weight ratio). [b] TS-1 with Si/Ti ratio of 30 was synthesized according to published procedure.[1]

TABLE 4: Catalytic Activities in 2,3,6-Trimethylphenol Hydroxylation over MTS-9, Ti-MCM-41, and TS-1[a]

catalysts	phenol conversion (%)	TOF (h^{-1})	product selectivity (%)		
			trimethyl-hydroquinone	trimethyl-benzoquinone	others
MTS-9	18.8	7.4	66.7	21.1	12.2
Ti-MCM-41	4.1	1.4	25.5	69.8	4.6
TS-1[b]	1.2	0.3	71.1	17.6	11.3

[a] Reaction conditions: acetonitrile as a solvent, reaction temperature at 80 °C, trimethylphenol/H_2O_2 = 3/1 (molar ratio), reaction time for 4 h, catalyst/phenol = 5% (weight ratio). [b] TS-1 with Si/Ti ratio of 30 was synthesized according to published procedure.[1]

Furthermore, we observe that the selectivity for hydroquinonone and catechol over mesoporous and microporous catalysts is slightly different. In mesoporous titanosilicates of MTS-9, the selectivity for hydroquionone and catechol is 40% and 60%. In contrast, the selectivity for hydroquionone and catechol over TS-1 catalyst is 50% and 50%. The high selectivity for hydroquionone over TS-1 is assigned to the shape selectivity of microporous size.[6]

As compared with as-synthesized MTS-9, the calcined MTS-9 shows relatively low conversion (14.5%) although the conversion is still much higher than that of Ti−MCM-41 and Ti−HMS, which is related to the change in titanium species of the sample by calcination at 500 °C for 4 h.

Styrene Epoxidation. The catalytic activities of various titanosilicates in styrene epoxidation are presented in Table 3. Obviously, they are all very active, but the product selectivity is quite different. MTS-9 and TS-1 show the conversion at 56.4 and 54.6% and high selectivity for styrene epoxide products including styrene epoxide and phenylacetaldehyde at 57.3 and 71.0% (phenylacetaldehyde is a isomer of styrene epoxide).[26] However, Ti−MCM-41 shows the conversion at 48.3% with 100% selectivity for benzaldehyde. The big difference in product selectivity indicates that the reaction mechanism and route in this reaction between MTS-9 and TS-1 with Ti−MCM-41 is distinguishable, which is assigned to the difference for titanium species in these titanosilicate catalysts.

Hydroxylation of 2,3,6-Trimethylphenol. The catalytic activities of various titanosilicates in hydroxylation of 2,3,6-trimethylphenol are presented in Table 4. TS-1, Ti−MCM-41, and Ti−HMS show very low conversion at 1.2, 4.1, and 2.0%, respectively. Ti−MCM-41 and Ti−HMS are inactive because of the relatively low oxidation ability of Ti species in the amorphous wall of mesoporous materials, and TS-1 is also inactive because of the inaccessibility of the small micropores of TS-1 to the large diameter of a bulky molecule like 2,3,6-trimethylphenol. Interestingly, MTS-9 is very active for this reaction with a conversion of 18.8%, indicating that MTS-9 is an effective catalyst for the oxidation of bulky molecules. Moreover, the main product of trimethylphenol hydroxylation proceeded by one step is trimethylhydroquinone, which is a necessary intermediate for synthesis of vitamin E. Conventionally, the synthesis of trimethylhydroquione is relatively complex, which includes the reaction procedures of sulfonation, oxidation, and reduction of the aromatics.[27]

4. Disscusions

4.1 Hydrothermal Stability. Recently, hydrothermal stability of mesoporous materials has been paid much attention because of the request in industrial application, and several successful methods for increasing the hydrothermal stability are used such as increasing thickness of mesoporous wall,[11a] incorporation of heteroatoms into silicon sites of mesoporous wall,[28] and mesoporous wall containing zeolite primary and secondary building units (PBSU).[20] In this work, as compared with that of Ti−MCM-41 and SBA-15, the superior hydrothermal stability of mesostructured titanosilicates (MTS-9) is related to the following factors: (1) thicker mesoporous wall, (2) incorporation of Ti into silicon sites, and (3) zeolite-like primary and secondary building units in mesoporous wall. These factors are well confirmed by experimental results. Both samples of MTS-9 and SBA-15 are synthesized in the same condition, giving almost the same mesopore size (Table 1), but the mesoporous wall of MTS-9 is 1.2 nm thicker than that of SBA-15 (MTS-9 and SBA-15 show (100) value at 9.2 and 11.0 nm, respectively, Figures 1 and 2). Generally, free titanium (Ti^{4+}) could not enter the framework of SBA-15 in conventional direct synthesis in strongly acidic media (pH <1). In our case, we directly introduce Ti into mesostructure in such a strong acidic media. The incorporation of Ti into the mesoporous wall possibly increases hydrothermal stability of these mesostructured titanosilicates.[20,21] It has been reported that amorphous nature of mesoporous wall is one of the most important factors for relatively low hydrothermal stability of mesoporous materials.[16] Obviously, introduction of zeolite primary and secondary building units into mesoporous wall increases the hydrothermal stability of mesoporous materials significantly. MTS-9 exhibits a clear band at 556 cm^{-1} (Figure 8), which is characteristic of five-membered rings of T−O−T (T = Si or Ti) in microporous crystals of TS-1 zeolite.[23] This confirms the existence of TS-1 primary and secondary building units in mesoporous wall of MTS-9.

4.2 Titanium Sites in As-Synthesized Mesostructured Titanosilicates. As observed in Tables 2−4, as-synthesized mesostructured titanosilicates such as MTS-9 exhibits very high activity in catalytic oxidations of both small molecules such as phenol and styrene and bulky molecules such as 2,3,6-trimethylphenol, which are reasonably assigned to their unique titanium sites in mesoporous wall of these mesostructured titanosilicates. The following evidence strongly argues that titanium sites in as-synthesized mesostructured titanosilicates are similar to those in zeolite TS-1.

(1) UV−visible spectroscopy and UV−Raman spectroscopy are very effective for characterizing titanium species in titanosilicates.[10,16,25] In these characterizations, as-synthesized MTS-9 has shown bands very close to those of TS-1 suggesting that the coordinated environment of titanium species in as-synthesized MTS-9 and TS-1 is very similar. In comparison, Ti−MCM-41 exhibits bands distinguishable with those of TS-1, indicating that the titanium species between MTS-9 and TS-1 with Ti−MCM-41 are quite different.

(2) In phenol hydroxylation by H_2O_2, mesostructured titanosilicates such as MTS-9 exhibit similar catalytic conversions with that of TS-1, which is much higher than that of Ti−MCM-

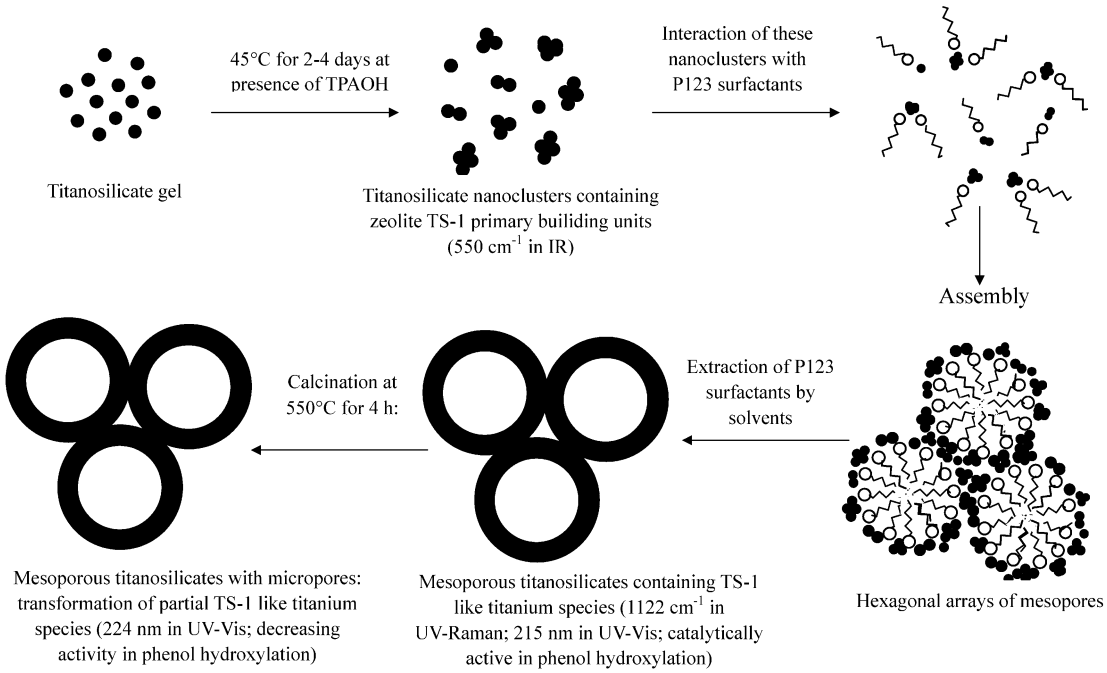

Figure 12. Proposed mechanism for the formation of ordered mesoporous titanosilicate of MTS-9.

41 and Ti−HMS (Table 2). In styrene epoxidation by H_2O_2, MTS-9 exhibits similar catalytic conversion and selectivity with those of TS-1. In comparison, Ti−MCM-41 shows quite different product selectivity, giving 100% selectivity for benzaldehyde. These results suggest that titanium species in MTS-9 and TS-1 are very similar, while the titanium species in Ti−MCM-41 and TS-1 are distinguishable.

In sum, all the above observations suggest that titanium species in mesostructured titanosilicates assembled from preformed titanosilicate precursors are zeolite TS-1-like, which are quite different from those of Ti−MCM-41 with amorphous nature of mesoporous wall. Further investigation is in progress in an effort to achieve unambiguous, preferably micrographic, identification and characterization of the micropore structures in the MTS-9 materials.

4.3 Titanium Sites in Calcined Mesostructured Titanosilicates. Stability of titanium species in mesostructured titanosilicates, particularly stability of titanium species in mesostructured titanosilicates for heating at 500−600 °C for several hours, is very important, because the heating at 500−600 °C for several hours for oxidation catalysts is an important procedure for the regeneration of the catalysts. Table 2 presents that calcined MTS-9 shows much lower conversion than that of as-synthesized MTS-9, although MTS-9 exhibits much higher activity than that of Ti−MCM-41. These results indicate the relatively low stability of mesostructured titanosilicates, and even heating at 500 °C for 4 h leads to the transformation of titanium species in the mesoporous wall. The suggestion is further confirmed by UV−visible spectroscopy (Figure 10). As-synthesized MTS-9 exhibits UV−visible band at 215 nm (Figure 10A), but calcination of as-synthesized MTS-9 shows UV−visible band at 224 nm (Figure 10C). Therefore, increasing thermal stability of TS-1-like titanium species in the mesoporous wall is still a great task for preparation of mesostructured titanosilicates.

4.4. Preformed Titanosilicate Precursors. The observed superior hydrothermal stability and high catalytic activity might be associated with our unique approach for the synthesis of the MTS-9 materials. It has been reported that chemical and physical properties of MCM-41, Ti−MCM-41, and SBA-15 are strongly dependent on the preparation conditions.[10,11,16] In MTS-9, the key point for the synthesis is, we believe, the preformation of titanosilicate precursors, which could undergo assembly with P123 micelle to generate mesostructures.

The titanosilicate precursors were prepared from heating titanosilicate gel in the presence of TPAOH at 100−140 °C for 2−3 h. TPAOH is a very good structure-directing agent in the synthesis of TS-1 zeolite.[1,6] We have obtained that addition of a small amount of titanosilicate precursors (3 wt %) into titanosilica gel ($TiO_2/SiO_2/Na_2O/H_2O$ = 1/10−40/2.8−12/500−900) at 140 °C for 2−4 h leads to TS-1 zeolite with high crystallization in the absence of organic templates.[30] The titanosilicate precursors appear to serve as seeds for the formation of TS-1 zeolite.[30] IR characterization of these titanosilicate precursors shows a clear band at 520−600 cm^{-1}, which is characteristic of five-membered rings. These results indicate that titanosilicate precursors contain zeolite primary and secondary structure building units.[30] Moreover, HR TEM observation of mesoporous wall shows some area in the walls of MTS-9 with micropores array (Figure 7). Similar phenomena have never been found in previous work on mesoporous materials.[31] The FFT diffractogram of these areas further confirms the periodical array of these micropores. We notice the size of these areas is about 2−3 nm, which is consistent with that of MFI nanoclusters (2.8 nm) reported by de Moor.[32] We think they are visual indication of preformed TS-1 nanoclusters embedded in the walls of MTS-9. On the basis of all these observations, we propose a tentative mechanism for the formation of mesoporous MTS-9 materials via the self-assembly of titanosilicate precursors, as nanoclusters with zeolite primary and secondary structure building units, with P123 micelle as illustrated in Figure 12.

We propose that during the preparation of MTS-9, the titanium sites are fixed in the framework of the TS-1 nanoclusters in the first step and are introduced into the mesoporous structure when the nanoclusters self-assemble with the template in the second step. Because of the strong acidic condition in the second step, the nanoclusters prepared in the first step would not grow continuously into large crystals and the appearance of TiO_2 as a separate phase is avoided.

Since the titanosilicate precursors contain zeolite primary and secondary structure building units, the size of titanosilicate precursor particles (or nanoclusters) should be larger than that of SiO_4 or TiO_4 tetrahedron for constructing the walls of mesopores. As a consequence, the mesopore wall in MTS-9 is thicker than that in SBA-15, which is assembled from SiO_4 tetrahedrons. In addition, the large particle size of titanosilicate precursors in preparation of MTS-9 should have some rigidity for assembly with P123 micelle, which might lead to the reduction of mesoporous order. As shown in Figures 1 and 3, MTS-9 shows relatively low XRD peaks, indicating the low mesoporous order, as compared SBA-15.

Furthermore, we are currently carrying out further experiments to elucidate the mechanism and to explore the applications of this concept in the synthesis of other material systems.

5. Conclusions

Mesostructured titanosilicates have been successfully synthesized from the assembly of preformed titanosilicate precursors with polymer surfactant micelle. The materials exhibit highly hydrothermal stability as compared with most other mesoporous materials. Characterization results indicate that these mesostructured titanosilicates of MTS-9 have titanium species TS-1-like and that the mesoporous walls contain the primary and secondary building units similar to those in microporous crystal of TS-1 zeolites. In catalytic hydroxylation of 2,3,6-tri-methylphenol, MTS-9 materials show greater activity in comparison with microporous crystal of TS-1 and mesoporous materials of Ti−MCM-41.

Acknowledgment. This work was supported by NSFC (29825108, 20173022, 20121103), the State Basic Research Project (G2000077507), and "863" Project (2002AA321010).

References and Notes

(1) Taramasso, M.; Perego, G.; Notari, B. U.S. Patent 4410501, 1983.
(2) Tuel, Z. *Zeolites* **1995**, *15*, 236−242.
(3) (a) Serrano, D. P.; Li, H. X.; Davis, M. E. *Chem. Commun*. **1992**, 745−747. (b) Reddy, K. M. et al. *Catal. Lett*. **1994**, *23*, 175−187.
(4) (a) Camblor, M. A.; Corma, A.; Perez-Pariente, J. *Zeolite* **1993**, *13*, 82−87. (b) Camblor, M. A.; Constantini, A.; Corma, A.; Gilbert, L.; Esteve, P.; Martinez, A.; Valencia, S. *Chem. Commun.* **1996**, 1339−1440. (c) Blasco, T.; Camblor, M. A.; Corma, A.; Perez-Pariente, J. *J. Am. Chem. Soc*. **1993**, *115*, 11806−11813. (d) Corma, A.; Esteve, P.; Martinez, A.; Valencia, S. *J. Catal.* **1995**, *152*, 18−24.
(5) (a) Huybrechts, D. R. C.; De Bruycker, L.; Jabobs, P. A. *Nature* **1990**, *345*, 240−242. (b) Selvam, T.; Ramaswamy, A. V. *Chem. Commun*. **1996**, 1215.
(6) (a) Notari, B. *Structure−Activity and Selectivity Relationship in Heterogeneous Catalysis*; Grasselli, R. K., Sleight, A. W., Eds.; Elsevier: Amsterdam, 1991; 243−256. (b) Notari, B. *Catal. Today* **1993**, *18*, 163−172.
(7) Roberts, M. A.; Sankar, G.; Thomas, J. M.; Jones, R. H.; Du, H.; Chen, J.; Pang, W.; Xu, R. *Nature* **1996**, *381*, 401−404.
(8) Kresge, C. T.; Leonowicz, M. E.; Roth, W. J.; Vartuli, J. C.; Beck, J. S. *Nature* **1992**, *352*, 710−712.
(9) (a) Corma, A.; Navarro, M. T.; Perez Pariente, J. *Chem. Commun*. **1994**, 147−148.
(10) Blasco, T.; Corma, A.; Navarro, M. T.; Perez Pariente, J. *J. Catal.* **1995**, *156*, 65−74.
(11) (a) Zhao, D.; Feng, J.; Huo, Q.; Melosh, N.; Fredrickson, G. H.; Chmelka, B. F.; Stucky, G. D. *Science* **1998**, *279*, 548. (b) Morey, M. S.; O'Brien, S.; Schwarz, S.; Stucky, G. D. *Chem. Mater*. **2000**, *12*, 898. (c) Luan, Z.; Bae, J. Y.; Kevan, L. *Chem. Mater*. **2000**, *12*, 3202. (d) Bharat, L. N.; Johnson, O.; Sridhar, K. *Chem. Mater*. **2001**, *13*, 552. (e) Wu, P.; Tatsumi, T.; Komatsu, T.; Yashima, T. *Chem. Mater*. **2002**, *14*, 1657.
(12) (a) Tanev, P. T.; Chibwe, M.; Pinnavaia, T. J. *Nature* **1994**, *368*, 321−323. (b) Zhang, W.; Wang, J.; Tanev, P. T.; Pinnavia, T. J. *Chem. Commun.* **1996**, 979−980. (c) Zhang, W.; Froba, M.; Wang, J.; Tanev, P. T.; Wong, J.; Pinnavia, T. J. *J. Am. Chem. Soc.* **1996**, *118*, 9164. (d) Bagshaw, S. A.; Pinnavaia, T. J. *Chem. Commun.* **1996**, 220.
(13) Maschmeyer, T.; Rey, F.; Sankar, G.; Thomas, J. M. *Nature* **1995**, *378*, 159−162.
(14) Inagaki, S.; Fukushima, Y.; Kuroda, K. *Chem. Commun.* **1993**, 680.
(15) Koyano, K. A.; Tatsumi, T. *Chem. Commun.* **1996**, 145−146.
(16) Corma, A. *Chem. Rev.* **1997**, *97*, 2373.
(17) Maclachlan, M. J.; Coombs, N.; Ozin, G. A. *Nature* **1999**, *397*, 681.
(18) (a) Liu, Y.; Zhang, W. Z.; Pinnavaia, T. J. *J. Am. Chem. Soc*. **2000**, *122*, 8791. (b) Liu, Y.; Pinnavaia, T. J. *Angew. Chem., Int. Ed.* **2001**, *40*, 1255.
(19) (a) Zhang, Z.; Han, Y.; Zhu, L.; Wang, R.; Yu, Y.; Qiu, S.; Zhao, D.; Xiao, F.-S. *Angew. Chem., Int. Ed.* **2001**, *40*, 1258−1262. (b) Zhang, Z.; Han, Y.; Zhu, L.; Wang, R.; Yu, Y.; Qiu, S.; Zhao, D.; Xiao, F.-S. *J. Am. Chem. Soc*. **2001**, *123*, 5014−5021.
(20) (a) Han, Y.; Xiao, F−S.; Wu, S.; Sun, Y.; Meng, X.; Li, D.; Lin, S.; Deng, F.; Ai, X. *J. Phys. Chem. B* **2001**, *105*, 7963. (b) Han, Y.; Wu, S.; Sun, Y.; Li, D.; Xiao, F.-S.; Liu, J.; Zhang, X. *Chem. Mater*. **2002**, *14*, 1144−1148.
(21) Xiao, F−S.; Han, Y.; Yu, Y.; Meng, X.; Yang, M.; Wu, S. *J. Am. Chem. Soc*. **2002**, *124*, 888.
(22) Li, J.; Zhang, X.; Han, Y.; Xiao, F.-S. *Chem. Mater*. **2002**, *14*, 2536.
(23) (a) Breck, D. W. *Zeolite Molecular Sieves*; Wiley: New York, 1974. (b) Jacobs, P. A.; Derouane, E. G.; Weitkamp, J. *J. Chem. Soc., Chem. Commun*. **1981**, 591.
(24) (a) Zecchina, A.; Spoto, G.; Bordiga, S.; Ferrero, A.; Petrini, G.; Padovan, M.; Leofanti, G. *Stud. Surf. Sci. Catal.* **1991**, *69*, 251. (b) Ricchiardi, G.; Damin, A.; Bordiga, S.; Lamberti, C.; Spanò, G.; Rivetti, F.; Zecchina, A. *J. Am. Chem. Soc.* **2001**, *121*, 11409. (c) Bordiga, S.; Coluccia, S.; Lamberti, C.; Marchese, L.; Zecchina, A.; Boscherini, F.; Buffa, F.; Genoni, F.; Leofanti, G.; Petrini, G.; Vlaic, G. *J. Phys. Chem*. **1994**, *98*, 4125. (d) Lamberti, C.; Bordiga, S.; Arduino, D.; Zecchina, A.; Geobaldo, F.; Spanò, G.; Genoni, F.; Petrini, G.; Carati, A.; Villain, F.; Vlaic, G. *J. Phys. Chem. B* **1998**, *102*, 6382. (e) Zecchina, A.; Bordiga, S.; Lamberti, C.; Ricchiardi, G.; Scarano, D.; Petrini, G.; Leofanti, G.; Mantegazza, M. *Catal. Today* **1996**, *32*, 97.
(25) Li, C.; Xiong, G.; Xin, Q.; Liu, J.; Ying, P.; Feng, Z.; Li, J.; Yang, W.; Wang, Y.; Wang, G.; Liu, X.; Lin, M.; Wang, X.; Min, E. *Angew. Chem., Int. Ed.* **1999**, *38*, 2220.
(26) Kumar, S.; Mirajkar, S.; Paris, G.; Kumar, P.; Kumar, R. *J. Catal*. **1995**, *156*, 163.
(27) Meng, X.; Sun, Z.; Lin, S.; Yang, M.; Yang, X.; Jiang, D.; Xiao, F.-S.; Chen, S. *Appl. Catal. A* **2002**, *236*, 17.
(28) Shen, S.-C.; Kawi, S. *J. Phys. Chem. B* **1999**, *103*, 8870.
(29) Yang, Q.; Wang, S.; Lu, J.; Xiong, G.; Feng, Z.; Xin, Q.; Li, C. *Appl. Catal., A* **2000**, *194*, 507.
(30) Xu, X. M. D. thesis, Jilin University, China, 1988.
(31) Zhao, D.; Huo, Q.; Jiang, F.; Chmelka, B. F.; Stucky, G. D. *J. Am. Chem. Soc.* **1998**, *120*, 6024.
(32) De Moor, P. E. A.; Beelen, T. P. M.; van Santen, R. A. *J. Phys. Chem. B* **1999**, *103*, 1639.